

Room-Temperature Kinetics of Short-Chain Alkanethiol Film Growth on Ag(111) from the Vapor Phase

Luis M. Rodríguez, J. Esteban Gayone,[†] Esteban A. Sánchez, and Oscar Grizzi

Centro Atómico Bariloche-CNEA, Instituto Balseiro-UNC, CONICET, 8400 S.C. de Bariloche, Río Negro, Argentina

Bárbara Blum* and Roberto C. Salvarezza

INIFTA, Departamento de Química, Universidad Nacional de La Plata y CONICET, Calle 64 y Diag. 113, Sucursal 4, Casilla de Correo 16, B1904DPI La Plata, Buenos Aires, Argentina

Received: March 2, 2006

We have used time-of-flight (TOF) direct recoiling spectroscopy (DRS) to follow propanethiol adsorption at 300 K from the vapor phase on an Ag(111) surface, for exposures ranging from 10^{-1} to 10^5 L. Results show that the adsorption proceeds with changes in the sticking coefficient, consistent with at least three phases. At low exposures, the alkanethiol molecules adsorb with high probability at defect sites, followed by a slower growth mode that essentially covers the whole surface. A third change in the sticking coefficient is associated with the final saturation stage, corresponding to a thicker layer related to molecules in a more upright orientation. The adsorption kinetics for hexanethiol is similar to that of propanethiol but taking place at higher rates, stressing the importance of the hydrocarbon chain length in the growth process. ISS-TOF measurements during thermal desorption show that most of the C, H, and S go away together, suggesting that the molecules adsorb and desorb from flat regions without S–C bond cleavage. Fitting the desorption maximum at 450 K with a first-order desorption curve gives a desorption energy of 1.43 eV. A small final S content that is correlated with the initial Ag(111) surface roughness is observed after desorption.

Self-assembled monolayers (SAMs) of *n*-alkanethiols ($\text{CH}_3-(\text{CH}_2)_{n-1}\text{SH}$; *C_n* hereafter) on metals are of great interest, because they provide an easy method to create surfaces with specific chemical functionalities in a controllable way.¹ These layers can be used in electronic devices, as building blocks for biosensors and molecular recognition, as ultrathin films for corrosion protection, and as anti-adherent and lubricant elements.¹ The formation of defect-free, dense, and stable surface structures can be a primary requirement for the use of *C_n* SAMs in these applications. This objective is not an easy task due to the formation of disordered, metastable phases along the self-assembly process. The SAM defects such as domain boundaries and molecular vacancies, the existence of substrate defects such as steps, and the formation of substrate vacancy- or ad-islands produced during *C_n* adsorption also contribute to disorder the layer. The smaller interchain interactions make these effects more important for short-chain ($2 \leq n \leq 6$) alkanethiols.

The control of SAM formation requires basic knowledge of the adsorption kinetics. Currently, there is detailed information about the different phases formed during alkanethiol adsorption on Au(111).² However, knowledge about the adsorption kinetics on Ag(111), the other paradigmatic substrate for alkanethiolate SAMs, is rather limited. The existence of two phases has been proposed both from a combined UPS–LEED study of dimethyl

disulfide adsorption³ and from electrochemical data, for short-chain alkanethiols on somewhat rougher Ag(111) surfaces.⁴ Recently, Yates et al. have shown that on Au(111)⁵ and Ag(110),⁶ short-chain *C_n* adsorb from vapors in ultrahigh vacuum (UHV) at low temperatures (*T*) without dissociation of the S–H bond, and the layers thus formed desorb below room *T*. On the other hand, exposure of Ag(111)⁷ and Au(111)⁸ to longer-chain alkanethiols ($n \geq 6$) at room temperature results in dense, ordered layers, but only after lengthy ($> 10\,000$ L) exposures.⁸ The dominance of adsorption at step-edges and other defect sites is well-established in electrochemical environments⁹ and has recently been shown to occur also in UHV experiments.⁵

In this work, we use time-of-flight direct recoiling spectroscopy (TOF-DRS)¹⁰ to study the adsorption of C3 at 300 K on a clean and smooth Ag(111) surface in UHV, for exposures ranging from 10^{-1} L to 10^5 L. We show that the kinetics of adsorption proceeds with changes in the sticking coefficient, consistent with at least three phases: *C_n* molecules at defect sites for very low coverages and highly tilted molecules on terraces at intermediate coverages preceding the formation of the saturation phase of more standing-up molecules. This sequence suggests a correlation between *C_n* adsorption on Ag(111) and Au(111).

Three aspects make TOF-DRS a useful tool for the observation of organic molecules at surfaces: (1) the high sensitivity to H atoms, normally not observed with electron spectroscopies, (2) the high efficiency of TOF techniques, that allows detection

* E-mail: bblum@inifta.unlp.edu.ar.

[†] E-mail: gayone@cab.cnea.gov.ar.

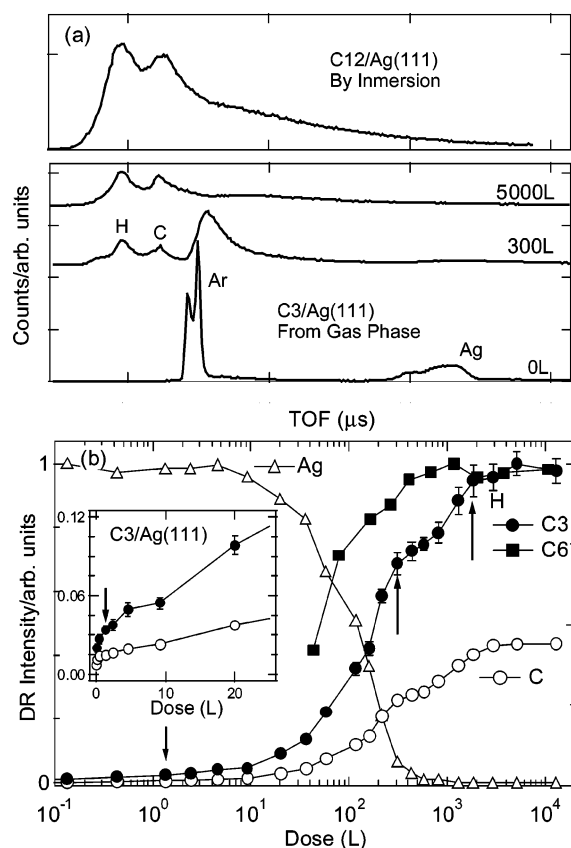


Figure 1. Upper panel: TOF-DRS spectra for clean and thiol-covered Ag(111) surfaces. Bottom panel: recoil intensities for Ag, H, and C vs C3 dose. The intensities of Ag and H peaks are normalized to 1. Inset: span of the lower range in linear scale. Arrows indicate major changes in sticking. Bars represent statistical errors. The H recoil intensity during C6 adsorption is also shown (full squares).

of both ions and neutrals, thus reducing the total amount of damage to very low levels, and (3) the possibility of obtaining information about the surface crystallography. The TOF technique also has a very high sensitivity to the topmost layer of atoms, a feature that is desirable to study functionalized molecules.¹¹ Details of the application of the technique to these organic systems will be described elsewhere.¹² Basically, in this technique, a pulsed ion beam (4.2 keV Ar^+) is used to bombard the surface at low incident angles (5° to 20°). The scattered projectiles together with the emitted surface atoms (neutrals plus ions, from both the adsorbed molecules and the substrate) were detected at a scattering angle of 45° , measured from the beam incidence direction, and analyzed by TOF-DRS techniques. TOF-DRS experiments were performed in a UHV chamber working at $(2\text{--}5) \times 10^{-10}$ Torr.

Smooth Ag(111) surfaces¹³ were obtained by repeated cycles of glancing sputtering ($2\text{--}3^\circ$) with 20 keV Ar^+ ions, while rotating the azimuthal angle continuously, followed by annealing at ~ 800 K. This procedure normally produces smoother surfaces than those prepared by low-energy Ar sputtering and annealing.¹⁴ The Ag(111) samples at 298 K were exposed in situ to C3 by backfilling the DRS chamber to pressures ranging from 10^{-9} to 10^{-5} Torr. The pressures were corrected by the ionization gauge sensitivities^{2b} (3.7 for C3; 7 for C6). The C3 (99%, Aldrich) was contained in a glass bottle that was connected to the vacuum chamber through a stainless steel leak valve. Further purification was obtained with several freeze-thaw-and-pump cycles.

Figure 1a shows characteristic TOF-DRS spectra for the clean Ag(111) surface, for the same surface exposed to C3 in vacuum,

and for another Ag(111) surface with a C12 layer grown by immersion. The clean surface spectrum shows the peaks of Ar single and multiple scattering off Ag, together with the Ag recoil peak from the outermost layer. Adsorption of C3 results in the appearance of H and C recoils. Integral peak intensities are shown as a function of exposure in Figure 1b. With increasing exposure, H and C recoil intensities continue to increase, accompanied by a decrease in Ag recoil intensity, until it becomes negligible at about 300 L. The disappearance of Ag recoils for doses higher than 300 L indicates full surface coverage. However, at this point, further dosing results in broadening of H and C peaks with a smaller change in peak height, accompanied by a decrease in the Ar scattering, until about 3000 L, where saturation is obtained.

The plot of the integral intensities (Figure 1b) suggests different growth regimes with different sticking coefficients (delimited by arrows for clarity). The uptake curves of C3 and C6 are similar to those reported for C10^{8a} and C6^{8b} on Au(111). The inset shows the initial uptake of C3, with a very high sticking probability, followed by a region with sticking probability 10–40 times smaller. The coverage at which this first change in sticking is observed is much larger for rougher surfaces.¹² Therefore, the regime below 2 L can be associated with C3 adsorption at defect sites, in agreement with STM results on Au(111),^{5,9} where exposures of up to 5×10^{14} molecules cm^{-2} resulted in essentially no adsorption at 300 K.^{5b} These exposures are similar to those of the first points in our graphs. Increasing the exposures 100 times (above 100 L) initiates the formation of a thiol layer that covers, after further dosing, the whole surface. The narrow H and C recoil peaks superimposed on the well-defined background of surface recoils, together with the presence of the peak of Ar multiple scattering from Ag (see Figure 1), suggest that this layer is extremely thin; otherwise, the Ar scattering from the Ag substrate would also be suppressed, as occurs for the saturation phase. This thinner layer therefore corresponds to a highly tilted (possibly lying-down) phase. Between 300 and 3000 L, the recoil peaks become broader and the Ar scattering feature almost disappears, suggesting that, at saturation, a thicker layer of molecules in a less tilted (possibly standing-up) orientation covers the whole surface. Note that the spectrum measured for C3 at saturation is very similar to that measured for C12 prepared by immersion. The latter case corresponds to a complete and distorted ($\sqrt{7} \times \sqrt{7}$)R19.1° layer of almost standing-up molecules in trans conformation.^{1,2b} The 50° tilted^{2c} (“lying-down”) phase and 30° tilted (“standing-up”) phase reported for propanethiol on Au(111) would produce qualitatively similar feature changes in the respective spectra. For C3 on Ag(111), complete Ag shadowing was obtained only for smooth surfaces; rougher silver surfaces always showed some Ar scattering off Ag. S recoils were never clearly seen, indicating shadowing by the alkyl chain. Note that this means that the alkyl chains are above the S plane, but it gives little information about the actual alkyl-chain orientation. The S content in the layers was determined by AES and XPS in separate setups. For C6, each regime is obtained at a lower exposure than for C3, pointing to the importance of chain length in the growth process.

Desorption experiments add information about the organic layer. After exposing the Ag(111) surface to a high dose of C3, the sample temperature (T) was raised slowly, at ~ 1 K/min. TOF-DRS spectra were measured until signals of neither H nor C were detected (inset of Figure 2), which occurred near 475 K. The H and C intensities follow a similar T dependence (Figure 2). The derivative of the H recoil intensity curve vs T

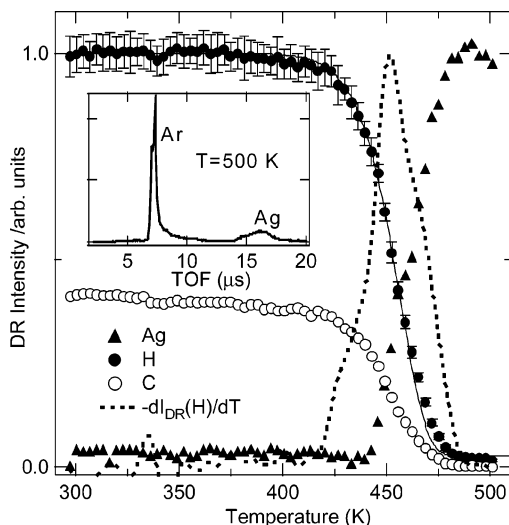


Figure 2. Ag, H, and C recoil intensities vs sample temperature. The full line is a fit to the H recoil intensity with a first-order desorption model. The derivative $-dI_{\text{DR}}(\text{H})/dT$ of the H data (dotted line) is included.

shows a desorption peak near 450 K. As will be described elsewhere, this desorption T depends on the initial coverage. Up to 425 K, there is little change in the surface coverage, the Ag recoil peak does not appear at these T , and only a small decrease in the H and C intensity is observed, probably associated with the disordering of the film but keeping the full surface covered. At 425 K, the onset for desorption takes place, revealing the substrate, and ends at about 475 K. This same desorption temperature range was observed for long-chain alkanethiolate SAMs prepared by immersion.¹⁵ By fitting the H-desorption experimental data with the Readhead equation (Figure 2) and using a frequency factor of 10^{13} s^{-1} ($5 \times 10^{11} \text{ s}^{-1}$)⁶ with a heating rate of 1 K/min, a desorption energy of 1.43 eV (1.30 eV) is obtained. This desorption energy is slightly larger than the value reported for chemisorbed alkanethiols on Au(111).¹⁶ The increased stability compares well with electrochemical data.¹⁷

The S detected at the end of the desorption process is very small, typically a few percent of monolayer, in agreement with recent results on Au(111)^{5b} and Ag(110).⁶ The final S-content increases with initial surface damage, suggesting that it takes place associated with defects, as in the case of Au(111).^{5b} The absence of any detectable amount of H or C associated with this S enables us to relate the S-species at defect sites with either sulfur or sulfides. Similar experiments performed with AES show a higher final S-content reflecting the higher damage imparted by the electron beam during spectra acquisition. The use of TOF-DRS combined with AES enables us to determine that C and H have the same dependence with T and most of the

S goes away, except for a small amount of S that is related to adsorption at defect sites. This suggests that the molecules adsorb and desorb on Ag(111) terraces without S–C bond cleavage, analogous to what has been observed on Cu(110) and Ag(110) after deuterating the alkanethiol molecules.⁶

Acknowledgment. We acknowledge fruitful discussions with Drs. M. L. Martiarena, P. Lustemberg, H. Ascolani, M. Sánchez, and G. Benitez, and financial support from FONCYT (PICT03 14452, PICT02 11111, PICT03 17492, PICT04 25959, PME-118), Fundación Antorchas, CONICET (PIP 5248), and Universidad Nac. de Cuyo (P no. 06/C202). This research was performed within the framework of the Argentine network of “Nanociencia y nanotecnología molecular, supramolecular e interfaces”.

References and Notes

- (1) (a) Love, J. C.; Estroff, L. A.; Kriebel, J. K.; Nuzzo, R. G.; Whitesides, G. M. *Chem. Rev.* **2005**, *105*, 1103–1170. (b) Ulman, A. *Chem. Rev.* **1996**, *96*, 1533–1554.
- (2) (a) Poirier, G. E.; Pylant, E. D. *Science* **1996**, *272*, 1145–1148. (b) Schreiber, F.; *Prog. Surf. Sci.* **2000**, *65*, 151–256. (c) Barrera, E.; Palacios-Lidón, E.; Munuera, C.; Torrelles, X.; Ferrer, S.; Jonas, U.; Salmeron, M.; Ocal, C. *J. Am. Chem. Soc.* **2004**, *126*, 385–395. (d) Vericat, C.; Vela, M. E.; Salvarezza, R. C. *Phys. Chem. Chem. Phys.* **2005**, *7*, 3258–3268.
- (3) Miller, A. D.; Gaffney, K. J.; Liu, S. H.; Szymanski, P.; Garrett-Roe, S.; Wong, C. M.; Harris, C. B. *J. Phys. Chem. A* **2002**, *106*, 7636–7638.
- (4) Hatchett, D. W.; Uibel, R. H.; Stevenson, K. J.; Harris, J. M.; White, H. S. *J. Am. Chem. Soc.* **1998**, *120*, 1062–1069.
- (5) (a) Maksymovych, P.; Sorescu, D. C.; Dougherty, D.; Yates, J. T., Jr. *J. Phys. Chem. B* **2005**, *109*, 22463–22468. (b) Rzeznicka, I. I.; Lee, J.; Maksymovych, P.; Yates, J. T., Jr. *J. Phys. Chem. B* **2005**, *109*, 15992–15996.
- (6) Lee, J. G.; Lee, J.; Yates, J. T., Jr. *J. Phys. Chem. B* **2004**, *108*, 1686–1693.
- (7) Rieley, H.; Kendall, G. C.; Jones, R. G.; Woodruff, D. P. *Langmuir* **1999**, *15*, 8856–8866.
- (8) (a) Schreiber, F.; Eberhardt, A.; Leung, T. Y. B.; Schwartz, P.; Wetterer, S. M.; Lavrich, D. J.; Berman, L.; Fenter, P.; Eisenberger, P.; Scoles, G. *Phys. Rev. B* **1998**, *57*, 12476–12481. (b) Kondoh, H.; Kodama, C.; Sumida, H.; Nozoye, H. *J. Chem. Phys.* **1999**, *111*, 1175–1184.
- (9) Vericat, C.; Andreasen, G.; Vela, M. E.; Martín, H.; Salvarezza, R. C. *J. Chem. Phys.* **2001**, *115*, 6672–6678.
- (10) Rabalais, J. W. *Principles and Applications of Ion Scattering Spectrometry. Surface Chemical and Structural Analysis*; Wiley-Interscience: New York, 2003.
- (11) Houssiau, L.; Graupe, M.; Colorado, R., Jr.; Kim, H. I.; Lee, T. R.; Perry, S. S.; Rabalais, J. W. *J. Chem. Phys.* **1998**, *109*, 9134–9147.
- (12) Rodríguez, L. M.; Gayone, J. E.; Sánchez, E. A.; Ascolani, H.; Grizzi, O.; Sánchez, M.; Blum, B.; Benitez, G.; Salvarezza, R. C. *Surf. Sci.* Submitted for publication.
- (13) MaTecK GmbH 99.99% purity. AFM yielded final rms height variations lower than $0.7 \text{ nm} \cdot \mu\text{m}^{-2}$.
- (14) Gayone, J. E.; Pregliasco, R. G.; Gómez, G. R.; Sánchez, E. A.; Grizzi, O. *Phys. Rev. B* **1997**, *56*, 4186–4193.
- (15) (a) Heinz, B.; Morgner, H. *Surf. Sci.* **1997**, *372*, 100–116.
- (16) Lavrich, D. J.; Wetterer, S. M.; Bernasek, S. L.; Scoles, G. *J. Phys. Chem. B* **1998**, *102*, 3456–3465.
- (17) Azzaroni, O.; Vela, M. E.; Andreasen, G.; Carro, P.; Salvarezza, R. C. *J. Phys. Chem. B* **2002**, *106*, 12267–12273.